Interdisciplinary Physics of the Sun

Spanish-German WE-Heraeus-Seminar

29 June – 04 July 2025

at the Physikzentrum Bad Honnef, Germany

Poster Presentation

Radial and Latitudinal Structure of the Solar Sphere: Evidence for Icosahedral Symmetry?

Jean-Guillaume RICHARD

Independent Scholar. 6, rue Guesnault, 41100 Vendome, France

Wilhelm und Else Heraeus-Stiftung

Fig. 1. **Meridional Cut of the Solar Sphere**

(vertical line: rotation axis; horizontal line: equator)

***r* 1 : Observed Top of the Sun's Central Fusion-Reaction Zone, defined as the Outward limit of Fusion Reactions (> 99.9%): 0.30 to ≈ 0.315... $R_\odot$ (black dashed circle):**

≈ 63° of the Sun's mass is below this radial limit.

$R_\odot$: Observed Top of Sun's Convective Envelope: defined as the Photosphere

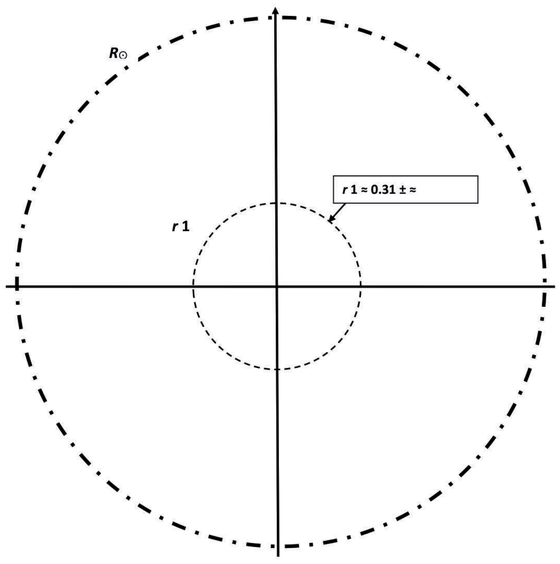

[1] Villante & Serenelli (2021): r = 0.3 $R_\odot$, and Fig 5 : $r \leq 0.315\ R_\odot$

[2] Bahcall, Serenelli, Basu (2005): $r \leq 0.315\ R_\odot$.

Fig. 1 bis. **Two Indistinguishable Radii, Given the Measurement Uncertainties:**

***r* 1 : Observed Top of the Sun's Central Fusion-Reaction Zone, defined as the Outward limit of Fusion Reactions (> 99.9%), black circle as in Fig. 1, 0.30 to ≈ 0.315... $R_\odot$, masked by:**

***r* 1 ico (Red circle): Top of the Central Sphere with Radius = 0.3108... (masks the black dashed circle in Fig. 2), nested in the Spherical-Code (Icosahedral) Spherical Packing Circumscribed by a Sphere S with radius = 1 (Pauling, 1947) [3].**

$R_\odot$ = 1: Observed Top of Sun's Convective Envelope, defined as the Photospheric radius.

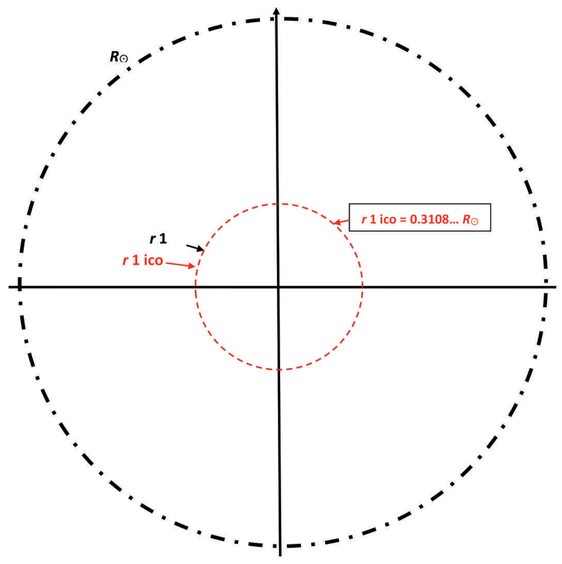

ABSTRACT

Radial and Latitudinal Structure of the Solar Sphere: Evidence for Icosahedral Symmetry?

Jean-Guillaume RICHARD

Independent Scholar. 6, rue Guesnault, 41100 Vendome, France

The radius r_1 of the energy-generating solar core is constrained to be ≈ 0.30 R_{SUN} based on neutrino detections [1], or up to ≈ 0.315 R_{SUN} in some standard solar models [2].

The radius r_2 of the fully radiative zone with *fully* rigid rotation, based on helioseismological measurements by MDI and HMI, is 0.65 ± 0.01 R_{SUN} [4].

These two radii are consistent with a three-layer radial structure with icosahedral symmetry within the circumscribing sphere with radius R, verified for exactly r_1 = 0.3108… R and r_2 = 0.6554… R [3].

A central sphere with radius r_1 is tangential to twelve spheres with radius r' = 0.3445…. R : two hemispheric sets consisting of a polar sphere and five "toroidal" spheres in a plane perpendicular to the polar axis. The centers of the "toroidal" spheres lie at latitude ± $\tan^{-1}(1/2)$ = ± 26.56...° vs. the equator [7]. In the Sun, ≈ 26.6° is the typical latitude of the first sunspots at sunspot minimum [13-15].

In the icosahedral geometry, in each hemisphere an axial cone is defined at latitude 58.28…° by the circle threading the tangential points between the five "toroidal" spheres. In the conical isorotation surfaces inferred from measurements by MDI and HMI in the bulk of the convective zone, the only radial meridional isotach i_{rad} is at 58° ± 2° latitude [8]. This demarcation line between two differential-rotation regimes with opposite gradients is approximately superposed with the variable boundary of unipolar caps at 55°-60° [10-11].

Yet, in GONG inversions, i_{rad} > 61° latitude [6] and r_2 < 0.63 R_{SUN} [6].

Meridional View | Polar View

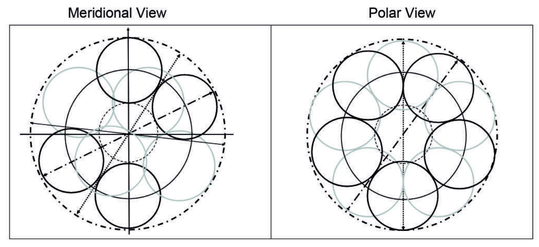

Fig. 2. **THE FUSION-FREE AND FULLY-RIGID SOLAR LAYER: Depth = *r* 2 - *r* 1**

***r* 1 : Observed Top of the Sun's Fusion-Reaction Zone**

***r* 2 : Observed Top of the the Fusion-Free and Fully Rigidly-Rotating Solar Layer:**

≈ 97° of the Sun's mass is below this limit, if it is at ≈ 0.65 $R_\odot$.

Helioseismologically-determined inward radial limit of ΔΩ:

No divergence as a Function of Radius, in Cuts at Constant Latitude 0°, 15°, 30°, 45°, 60°.

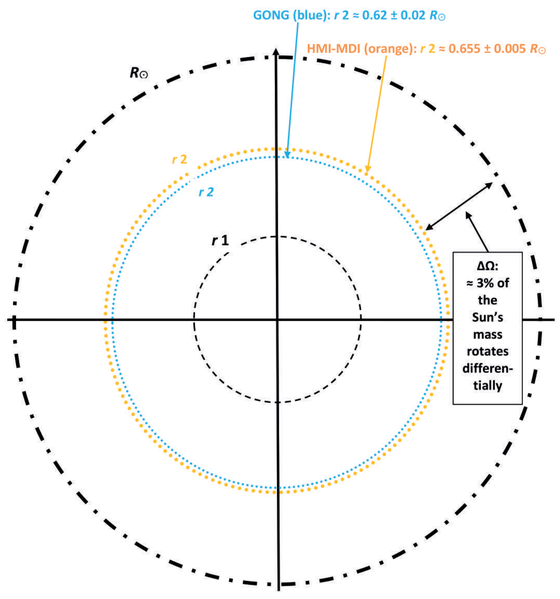

HMI-MDI. [4] Schad & Roth (2020): "about 0.65" $R_\odot$.

[5] Rozelot, Kosovichev, Kitiashvili (2024), Fig. 1 c. : ≈ 0.655 $R_\odot$, "averaged over all MDI and HMI measurements in 1996-2024".

GONG. [6] Howe (2009. LRSP,6.1: Solar Interior Rotation. Fig. 19 (right): ≈ 0.625 $R_\odot$. ["Adapted from Howe et al. (2000b)" (*Science*, 2000,5462)] (updates > 2009 ?)

Fig. 2 bis. **Comparison with**

The radius of the Circle threading the Centers of the Twelve Packed Spheres

***r* 2 ico : radius of the Circle which is the Meridional cut of the Spherical Surface threading the Centers of the Spheres kissing the Central Sphere in the Spherical-Code Packing (*r* 2 ico masks the HMI-MDI circle in Fig. 2).**

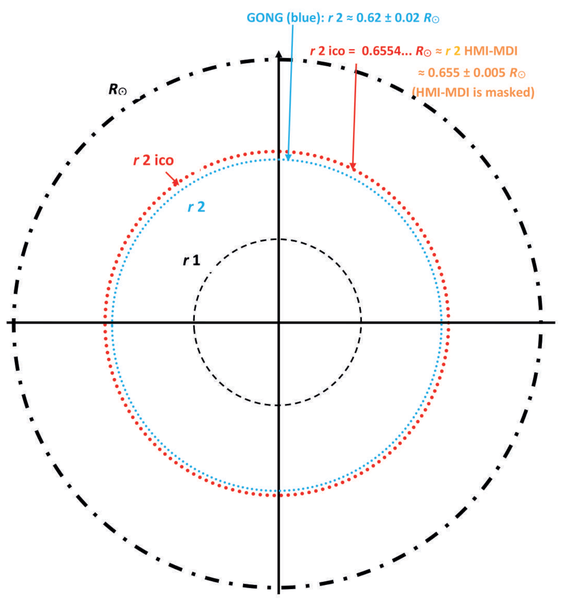

Fig. 2 ter. **TWO REMAINING PROBLEMS WITH STANDARD SOLAR MODELS:**

"Acoustic Glitch", and Lithium Depletion

***r* 2 : Observed Top of the the Fusion-Free and Fully Rigidly-Rotating Solar Layer.**

***r* 2 ico : radius of the Circle which is the Meridional cut of the Spherical Surface threading the Centers of the Spheres kissing the Central Sphere in the Spherical-Code Packing (masks the HMI-MDI circle in Fig. 2).**

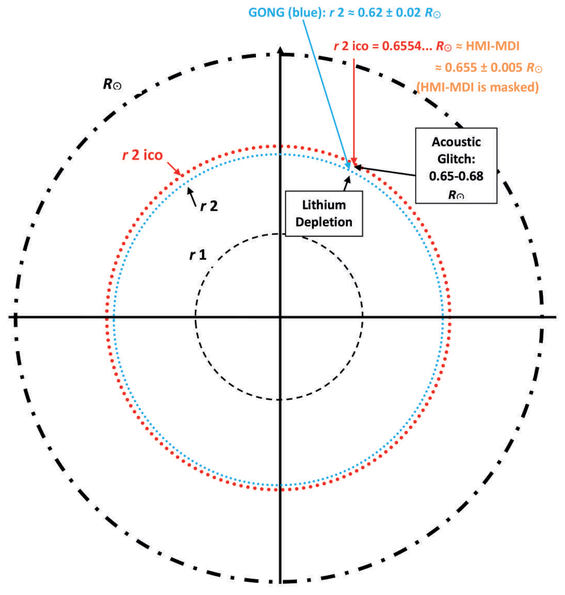

The Polar Icosahedral Configuration (J.-G. Richard)

applied to Schütte and Van Der Waerden (1953)'s [7] Sphere Packing

(Polar view of a 3D model, three pictures; see also: Optimal Spherical Code)

- **Top**: **entire model**, twelve peripheral equal spheres, mutually tangent by pairs.
- **Middle**: **northern hemisphere (NH), Bottom**: **southern hemisphere (SH)**. The five toroidal spheres around the polar sphere in the middle, atop in NH and at the bottom in SH, are in a plane parallel to the equator of the circumscribing sphere S.

In the bottom picture one can see, above the SH polar sphere, the open **central cavity** fitting a spherical **core** with radius equal to $\sqrt{\frac{2\sqrt{5}}{\sqrt{8}-1}} - 1$ = 0.902... times the radius of each of the twelve spheres packed around it (Pauling, 1947) [3].

Interlocking Sphere Packing

The SH five-sphere ring is offset by 36° in longitude vs. the NH ring, allowing the close packing in which SH toroidal spheres lock with the NH spheres in five hemispheric longitudinal interstices. The five toroidal spheres in one hemisphere thus overlap in latitude by 5.15…° into the opposite hemisphere.

No Hemispheric Mirror Symmetry: The Anti-Dynamo Theorem does not Apply?

Thus, there is no hemispheric mirror-symmetry in the configuration. In the case of a circumscribing stellar spheroid such as the photosphere, the Cowling anti-dynamo theorem thus might not apply.

Fig. 3. **HMI/MDI Radial Isotach (Observed range), GONG Radial Isotach (Observed range) and Icosahedral Central-Angle Radial Line (l_{RAD})**

- Blue rectangle: observed range in GONG inversions for the latitude of the radial isotach

- Brown rectangle: observed range in HMI and MDI inversions

- Red solid line in the CZ at 58.28...° latitude = 90° - (63.43° / 2): Icosahedral Central-Angle Radial Line l_{RAD} . It is also defined in the Spherical-Code Packing by the tangential point between a polar sphere and each of the five equal spheres surrounding it.

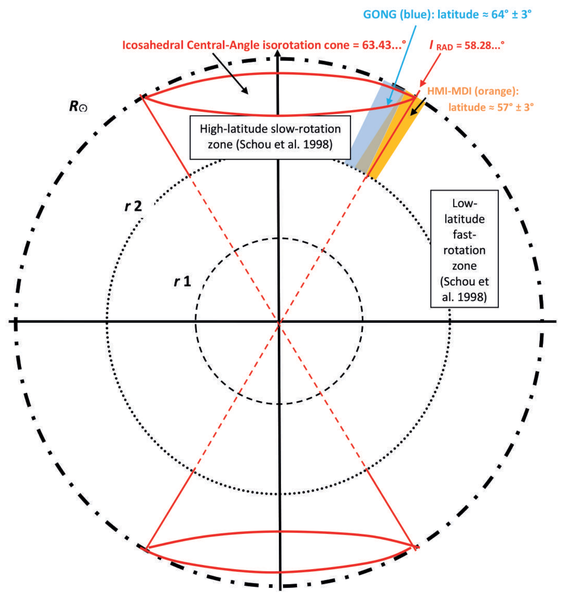

MDI, HMI: E.g. : [8] Larson, T., and Schou, J. 2018, *Solar Phys.*, 293(2) (2018). Figures 29 and 30. MDI (1996-2010), HMI (2010-2017).

GONG (1996-1999). E.g. [6] Howe (2009): LRSP,6.1: Solar Interior Rotation. Fig. 19 (left): 65°. (updates?)

Fig. 4. **Differential Rotation Pattern in the Bulk of the CZ:**

Where is the Radial Isotach, if Any?

Cartoons of four idealized overall patterns (0°-90° latitude quadrant) of the rotation profile in the bulk of the CZ (eight isotachs, each), in a meridional cut of isorotation surfaces:

- Top Panel: Helioseismically-Determined Isotachs: a) Inward-divergent; (b) 25°-slant.

- Bottom Panel: Isotachs commonly assumed in Dynamo Simulations: (c) Outward-divergent: all-radial case ("spoke-like"); (d) Axis-parallel ("cylindrical", no radial isotach).

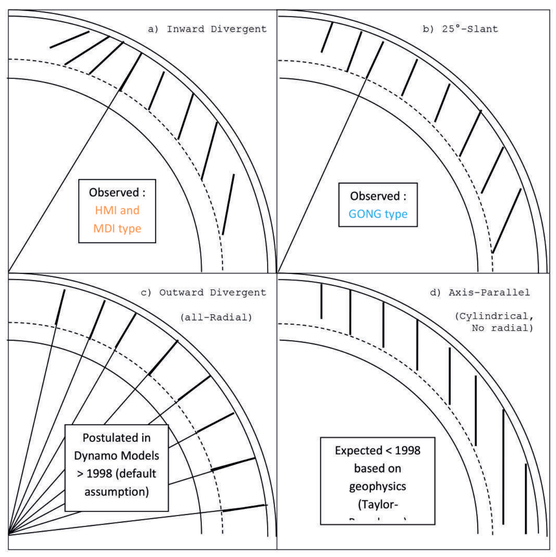

Dashed circle-quadrant: 0.80 $R_\odot$ (interior limit of quasi-rectilinear isotach segments).

Solid circle-quadrants: 1 $R_\odot$, 0.95 $R_\odot$, and 0.72 $R_\odot$.

Thick solid lines: quasi-rectilinear isotach segments.

Thin straight radial solid line from the center: radial direction of the radial isotach, if any.

Fig. 5. **Solar-Surface Magnetic Field: Unipolar vs. Bipolar Boundary**

Schou et al. (1998) [9] first suggested a connection between: the slow vs. fast rotation boundary in the bulk of the CZ, and the Unipolar vs. Bipolar magnetic -field boundary at the photosphere.

- Black: Common Estimates of the Time-Weighted Typical Latitude of the Varying Boundary of the Surface Magnetic Field: Predominantly Unipolar vs. Predominantly Bipolar.

- Red solid line in the CZ at 58.28...° latitude = 90° - (63.43° / 2): Icosahedral Central-Angle Radial Line l_{RAD}. It is also defined (see Fig. 6) in the Spherical-Code Packing by the tangential point between a polar sphere and each of the five equal spheres surrounding it.

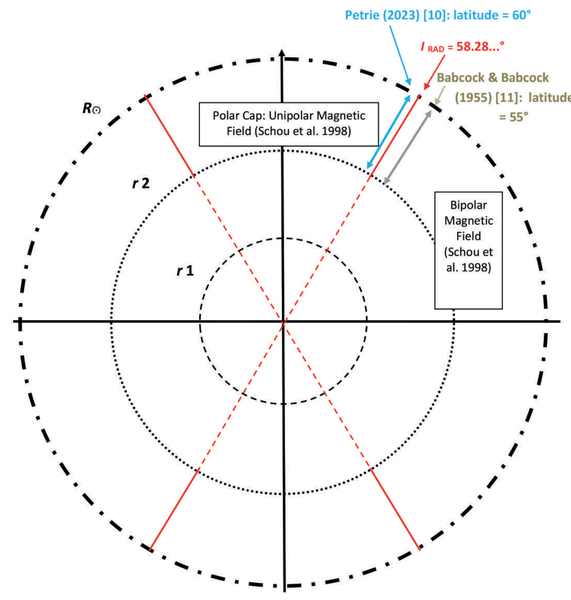

Icosahedral Reference Symmetry in Helioseismological Pipelines ?

E.g. : $\tan^{-1}\frac{1}{2}$ = **26.56...°**

Odd c splitting coefficients are sensitive to rotation.

Basu et al. (2024) [12]:

"The clearest signature of the tachocline is in the c_3 splittings"

BUT

« There is no contribution from c_3 at a latitude of approximately 26.56°"

(Vanishing value, given $\tan^{-1}\frac{1}{2}$ = 26.56...°, in Basu et al. (2024)'s equation (4))

Fig. 6. **Meridional View of the Polar Icosahedral Configuration**

Red: Meridional Cut through the Center of a Sphere S with radius $R_\odot$ and through the Centers of four Equal Spheres Circumscribed by Sphere S.

- Red solid line in the CZ at 58.28...° latitude = 90° - (63.43° / 2): Icosahedral Central-Angle Radial Line l_{RAD}. It is defined in the Spherical-Code Packing by the tangential point between a polar sphere and each of the five equal "toroidal" spheres surrounding it. The centre of each "toroidal" sphere is at tan $^{-1}$(1 / 2) = 26.56...° latitude vs. the equator of the circumscribing Sphere S.

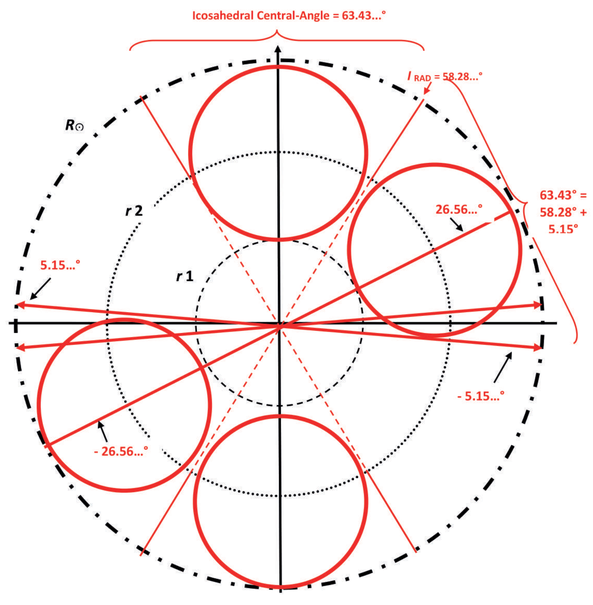

Fig. 6 bis. **Average Latitude of Sunspots over the Sunspot Cycle: Observations Compared with the Geometry of the Spherical-Code Packing**

Blue Arrows: Average Latitude of sunspots since 1874

- Arrow's Start, First New-cycle spots near Sunspot Minimum: ≈ ± 26.6° ([13] Jiang et al., 2011: 26.4°; [14] Ivanov and Miletsky, 2014: 26.6° ; [15] Leussu et al., 2017: 26.5°)

- Arrow's End: Last spots in a cycle: ≈ ± 5° ([16] Lockyer , 1903: sunspots "vanish about latitude ± 5°"; [17] Abetti, 1957: sunspots are "effectively contained beyond latitude ± 5°"; [18] Solanki et al., 2006: sunspots "reach about ± 5° average latitude towards the end of the cycle").

- Four Red circles: Meridional Cut through the Center of a Sphere S with radius $R_\odot$ and through the Centers of four Equal Spheres Circumscribed by S. The centre of each "toroidal" sphere is at tan $^{-1}$(1 / 2) = 26.56...° latitude vs. the equator of the circumscribing Sphere S.

- Red arrows intersecting Sphere S at ± 5.15...° latitude: hemispheric overlap in latitude, denoting the interpenetration interval between the two hemispheric rings of five Equal Spheres in the Spherical-Code packing (two red triangles, each symmetric about the equator).

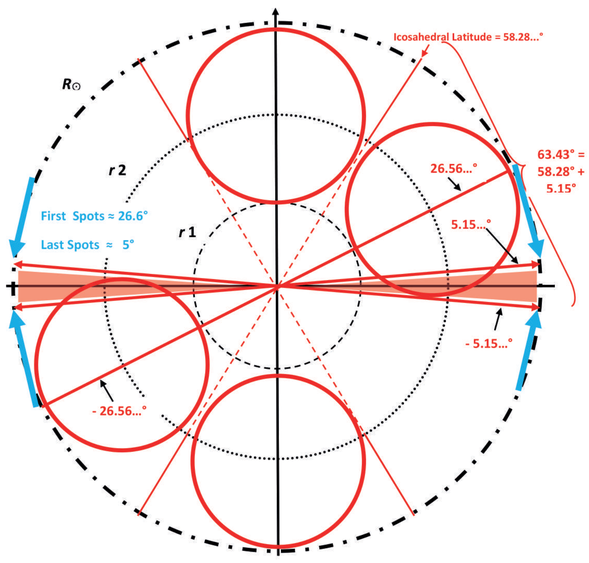

Fig. 7. **Polar View of the Polar Icosahedral Configuration:**

Two non-Mirror-Symmetric Hemispheric Toroids: Helmholtz Coil?

Tan $^{-1}$(1 / 2) = ± 26.56...° is the latitude of each toroid in a Helmholtz coil ("HC") circumscribed in a sphere, generating a homogenous dipole magnetic field such as, e.g., the solar axial dipole at sunspot minimum. Such a HC consists of two parallel current loops, one threading the center of each packed sphere in the northern hemisphere (NH), and the other one in the southern hemisphere (SH). The radius of each packed sphere is the radius of the circular cylinder circumscribing the five spheres in a five-sphere hemispheric ring, yielding two overlapping equator-parallel hemispheric toroids (Richard, 2025 [submitted]) [19].

In a polar view of the polar icosahedral Sphere-Packing Configuration, the SH five-sphere ring is offset by 36° in longitude vs. the NH ring, allowing the close packing in which SH toroidal spheres lock with the NH spheres in five hemispheric longitudinal interstices, with an overlap in latitude of 5.15...° into the opposite hemisphere.

No Hemispheric Mirror Symmetry: The Anti-Dynamo Theorem does not Apply?

Thus, there is no hemispheric mirror-symmetry in the configuration. In the case of a circumscribing stellar spheroid such as the photosphere, the Cowling anti-dynamo theorem thus might not apply. Differential rotation would provide the shear for self-excitation.

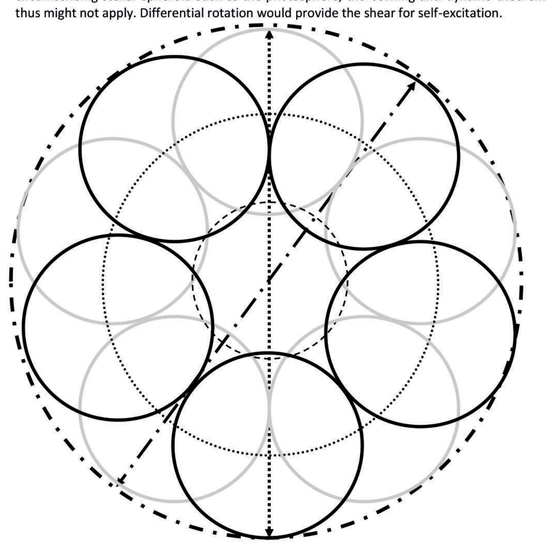

References

[1] Villante, F. L., and Serenelli, A., *Front. Astron. Space Sci.*, 7, 618356 (2021)

[2] Bahcall, J. N., Serenelli, A. M., and Basu, S. *Astrophys. J.* 621, L83 (2005)

[3] Pauling, L., *J. Amer. Chem. Soc.*, 69(3), 542 (1947)

[4] Schad and Roth, *Astrophys. J.*, 890(1), 32 (2020)

[5] Rozelot, J.-P., Kosovichev, A., Kitiashvili, I. *Astronomy in Focus.* Warral, D., ed. XXXIInd IAU General Assembly, August 2024 (arxiv: 2501.08021v2) (2025)

[6] Howe, R. *Living Reviews in Solar Physics*, 6(1) (2009)

[7] Schütte, K., and van der Waerden, B. L. *Math. Ann.*, 125, 325 (1953)

[8] Larson, T., and Schou, J. *Solar Phys.*, 293(2) (2018)

[9] Schou, J., et al., *Astrophys. J.* 505, 390 (1998)

[10] Petrie, G., *Solar Phys.*, 298.3, 43 (2023)

[11] Babcock, H. W., and Babcock, H. D. *Astrophys. J*, 121, 349 (1955)

[12] Basu, S., Andrade de Aguiar, W. A. M., and Korzennik, S. G. *Astrophys. J.* 975, 276 (2024)

[13] Jiang, J., Cameron, R. H., Schmitt, D., and Schüssler, M. *Astron. Astrophys.*, 528, A82 (2011)

[14] Ivanov, V. G., and Miletsky, E. V., *Geomagn. Aeronom.*, 54(7) (2014)

[15] Leussu, R., Usoskin, I. G., Senthamizh Pavai, V., Diercke, A., Arlt, R., Denker, C., and Mursula, K. *Astron. Astrophys.* 599, A131 (2017)

[16] Lockyer, W. S. J. *Observatory*, June, 236 (1903)

[17] Abetti, G. *The Sun*, Faber & Faber, London, p. 78 (1957)

[18] Solanki, S. K., Inhester, B., and Schüssler, M. *Reports on Progress in Physics*, 69(3), 563 (2006)

[19] Richard, J.-G. (submitted) (2025)